

1
2
3
4 Limiting Factors for Nomadic Pastoralism in Mongolian Steppe: A Hydrologic
5 Perspective
6

7
8 Michiaki Sugita^{1*}, Shintaroh Yoshizawa^{2**}, and Ishgaldam Byambakhuu^{2***}
9

10
11
12 ¹ Faculty of Life and Environmental Sciences, University of Tsukuba, Ibaraki 305-8572,
13 Japan

14 ² Graduate School of Life and Environmental Sciences, University of Tsukuba, Ibaraki
15 305-8572, Japan

16
17 * Corresponding author, sugita@geoenv.tsukuba.ac.jp

18 ** Now at Graduate School of Comprehensive Human Sciences, University of Tsukuba,
19 Ibaraki, Japan

20 *** Now at Department of Environmental Sciences and Chemical Engineering, School of
21 Engineering and Applied Sciences, National University of Mongolia, Ulaanbaatar,
22 Mongolia
23

24
25
26 The final publication is available at ScienceDirect via [http://dx.doi.org/
27 10.1016/j.jhydrol.2015.02.050](http://dx.doi.org/10.1016/j.jhydrol.2015.02.050)

28
29 © 2015. This manuscript version is made available under the CC-BY-NC-ND 4.0
30 license <http://creativecommons.org/licenses/by-nc-nd/4.0/>
31
32

33 Abstract

34

35 In this study, limiting factors for continuing nomadic pastoralism in steppe areas were
36 studied based on a hydrologic perspective. Two small watersheds in central Mongolia
37 were selected for an assessment of water balance and hydrologic processes. We
38 determined that the majority of annual precipitation, ~88-96 mm, was lost by
39 evaporation (82%) while only a small proportion went to groundwater discharge,
40 surface runoff, and groundwater consumption by nomadic activities. The soil column
41 was found to absorb large fluctuations in precipitation although its connection to
42 groundwater was very weak. Groundwater recharge was, therefore, very small and
43 occurred only rarely during heavy rainfall events in valley bottoms. However, current
44 water storage in shallow groundwater was determined to be quite sufficient for
45 continuing nomadic pastoralism when compared to the drinking water requirements of
46 livestock. The main limiting factors identified were a temporal lack of feed to animals
47 due to a loss of aboveground biomass resulting from soil moisture shortages during
48 drought conditions, and a decline in the number and maintenance level of the traditional
49 well network that, due to access to shallow groundwater, has allowed herders to migrate
50 to areas with better conditions in remote Mongolian steppe.

51

52 Keywords: water balance; groundwater recharge, nomadic pastoralism; steppe;
53 Mongolia

54

55 1. Introduction

56

57 In remote rangelands, water is often considered to be a limiting factor for
58 continued nomadic pastoralism because drinking water limitations influence the
59 sustainability of livestock. In most cases, with the exception of camels which can
60 survive for extended periods without drinking water, livestock must consume water on a
61 daily basis. Since perennial streams are rare to non-existent in many arid regions,
62 daily water consumption largely depends, with the exception of regions near mountains
63 where spring water is expected and the winter season when accumulated snow and ice
64 serve as a water, on shallow groundwater.

65 Since nomadic pastoralism has continued over centuries (e.g., Miyawaki, 2002;
66 Matsubara, 2005; Cribb, 1991), implying sustainability, the impact of livestock on
67 shallow groundwater stocks should not be very large. Crude estimates of annual water
68 balance support this assessment. For example, by assuming an annual rainfall value of
69 $P = 150$ mm, an evaporation value of $E = 0.8 \times P = 120$ mm, a daily water consumption
70 value for sheep of 4 L, and a typical stocking rate of 0.5 head/ha, an annual sheep water
71 consumption of 730 L/ha and an annual available water value ($=P-E$) of 3.0×10^5 L/ha
72 can be derived. Given these values, water consumption by livestock only constitutes
73 0.2% of available water. However, such an argument is based on average conditions.
74 A relevant question is whether or not water is sufficiently available everywhere and at
75 all times, and if not, what could induce a temporal/local water shortage. Additional
76 questions include the following: (i) Is water abundant in every season of the year? (ii)
77 Is there enough water even under drought conditions when annual rainfall is much less
78 than the climatic mean value? (iii) Is the stocking rate as low as the assumed value
79 everywhere? (iv) Will the stocking rate continue to be at the same level as the
80 assumed value? (v) Were stocking rates and water balance regimes different in the past?
81 Such questions address some of the relevant factors that could influence the
82 sustainability of nomadic pastoralism. To answer such questions, crude estimations
83 are not sufficient. A comprehensive study with more reliable data and statistics is
84 clearly required.

85 The above discussion presents a brief background for the present study. We
86 performed a detailed water balance and estimated hydrologic processes for pastureland
87 in order to shed some light on the limiting factors for nomadic pastoralism.
88 Additionally, vegetation dynamics in relation to the water deficit were considered by
89 referring to information presented in the companion study of Satoh et al. (2012), and
90 were based on detailed ecohydrologic observations and the carbon dynamic simulation

91 results of Chen et al. (2007), among others. Since a lack of water can also limit
92 nomadic pastoralism due to the influence of water availability on vegetation growth,
93 information on vegetation dynamics was also obtained. Combining water balance
94 estimates and ecohydrological information allowed us to answer the question of why
95 nomadic pastoralism has been able to continue over centuries under arid conditions.

96 When a water balance approach is applied for estimating minor hydrologic
97 components such as groundwater recharge rates, the resulting estimates tend to involve
98 a large error (e.g., Healy, 2010). Therefore, our estimations were not only based on the
99 water balance method but also on supplementary observations. Analyses were also
100 applied whenever possible in order to enhance the reliability of water balance estimates.
101 Two small watersheds located in the central portion of Mongolia were selected for our
102 analyses. Therefore, the work presented here is essentially a case study. However,
103 Mongolian steppe is a part of the largest rangeland belt on Earth, extending from
104 northeastern to Central Asia (Shiirevdamba, 1998), thus, our results should be
105 applicable to larger areas containing similar vegetation and topography.

106

107 2. Method

108 2-1. Study area

109 For the study, two small watersheds, W1 and W2, were selected within a gentle
110 hilly terrain in Saintsagaan soum (county) in Dundgobi aimag (prefecture), located
111 approximately 4 km northeast of the city of Mandalgobi in Mongolia (Fig.1). The
112 watershed area of W1 is $A = 3.3967 \text{ km}^2$ and that of W2 is $A = 11.3567 \text{ km}^2$ (see the
113 Appendix for watershed boundary determinations). The soil in this area is classified as
114 semidesert brown soil or semidesert brown friable sandy soil (Dorzgotov 2003). The
115 morphology of the A horizon can be characterized by high compactness, a brown color,
116 and weak development of the soil structure. A high sand and gravel content can also
117 be observed within the surface soil (Asano 2010, personal communication). The
118 bedrock is composed mainly of Permian felsic rocks such as dacite, rhyolite, or quartz
119 porphyry (Mineral Resources Authority of Mongolia, 2001; Mineral Resources
120 Authority of Mongolia and Mongolian Academy of Sciences, 1998). The climate is
121 classified as arid and has a mean annual precipitation of 150 mm (for 1944–2011), as
122 measured by the nearby meteorological station (located approximately 5.5 km southeast
123 from the study area) at the Research and Information Institute of Meteorology,
124 Hydrology and Environment (hereafter referred to as the IMH station). According to
125 the Standardized Precipitation Index (SPI) for three, six and 12 months, the observation
126 period from 2008-2011 can be classified as “near normal” to “moderately dry” (WMO,

127 2012). Approximately 78% of annual precipitation falls during the summer from
128 June-August. The mean annual air temperature is 1.5°C, while the annual range of
129 monthly means is as large as 37°C, with a low of -17.7°C in January and a high of
130 19.3°C in July.

131 According to the Mongolian vegetation classification scheme, the area is
132 located within a boundary zone between the desert steppe class and the steppe/dry
133 steppe class. Dominant vegetation consists of the C₃ herbaceous plant *Allium*
134 *polyrrhizum* and some dotted communities of the C₃ shrub *Caragana microphylla*.
135 However, during the study period, even during the typical growing season from May
136 through August, only intermittent appearances of *Allium* were observed at the surface
137 after rainfall events (also see Satoh et al., 2012). Plants in this area, especially *Allium*,
138 are under grazing pressure mainly from the sheep and goats of local nomadic herdsmen
139 (Byambakhuu et al., 2010, Satoh et al, 2012). The mean number of animals per unit
140 area (i.e., the grazing pressure or the stocking rate) in 2009 was $S_r = 0.79$ SEU ha⁻¹ for
141 Saintsagaan soum (3.39×10^3 km²) and $S_r = 0.35$ SEU ha⁻¹ for Dundgobi aimag
142 (7.47×10^4 km²), while, as determined from local animal population numbers (see
143 below), it was approximately $S_r = 0.56$ SEU ha⁻¹ within watersheds W1 and W2. SEU
144 is the sheep equivalent unit and represents the population sum for five major animal
145 types in Mongolia (sheep, goats, horses, cattle and cows, and camels) converted to
146 sheep equivalent numbers using common factors (e.g., Pratt and Rasmussen, 2001).
147 Thus, the average stocking rate for the two watersheds is between the higher S_r of
148 Saintsagaan soum and the lower value of Dundgobi aimag, implying that the target
149 study areas reflects a somewhat modified herding condition due to the proximity to the
150 city of Mandalgobi. However, conditions within the W1 and W2 watersheds represent
151 more of the conditions of rural rangelands in Mongolia than those in central portions
152 near its capital city of Ulaanbaatar where a $S_r \geq 1.25$ is often observed (see e.g., Fig. 12
153 of Sugita et al., 2007).

154 In and around the W1 and W2 watersheds, there are four wells (GW1-GW4)
155 completed in shallow groundwater (Fig.1) and were used regularly by one to two nomad
156 families, and infrequently by other families, during the observation period. A 'ger' (a
157 nomad tent) was placed near GW1 by one family during the summer of 2009. Another
158 family camped throughout the year near GW2. These types of wells are used to obtain
159 access to shallow groundwater and are the main water resource used by local herdsmen
160 for daily life. More specifically, the GW1 well (with a depth of 5.5 m; where the
161 typical water depth is 0.5 m) was only used regularly during the summer season of 2009
162 by one family, while from 2010 it was only periodically visited and used by nomads

163 from the W2 watershed. Wells GW2 (with a depth of 3.1 m and a water depth of 0.5
164 m) and GW4 (with a depth of 1.7 m and a water depth of 0.2 m) were used throughout
165 the year by this family. The GW3 well (with a depth of 2.1 m and a water depth of 0.1
166 m) did not provide sufficient water and was not normally used by the nomad families.

167 The surface located 50-100 m from the wells and the 'ger' was essentially bare
168 ground without vegetation, a result of micro-scale overgrazing. Such concentrated
169 overgrazing is common in this area of Mongolia but generally disappears or decreases
170 exponentially from 50-100 m as distance from the source point of grazing, such as a
171 well, increases (e.g., Sasaki et al., 2008). Therefore, the extent of such bare ground is
172 only limited to areas surrounding wells and 'gers' and, thus, impacts to watershed-scale
173 water balances and hydrologic processes can likely be ignored.

174

175 2-2. Estimations of water balance components

176 The water balance of a watershed for a given period can be expressed with a
177 dimension of $[LT^{-1}]$, as follows:

178

$$179 P = E + G_{out} + R_{out} + U + \Delta S \quad (1)$$

180

181 where P is precipitation, E is evaporation (soil evaporation and transpiration), G_{out} is
182 groundwater discharge from the watershed, R_{out} is surface runoff from the watershed, U
183 is the amount of groundwater extracted through the wells used mainly for grazing, and
184 ΔS is the storage change within the watershed over the period in which (1) is determined.
185 In the present study, (1) was considered from the surface down to the bottom of the
186 shallow, unconfined aquifer and we assumed that the shallow aquifer is underlain by an
187 impermeable layer so no leakage occurs. Since the observed groundwater level did not
188 show steady declines during the dry period (see the Results section and the Appendix),
189 such an assumption is likely acceptable.

190 Although the exact thickness of the shallow aquifer is unknown, the Well
191 Database of Mongolia, currently being compiled by the IMH (Davaa, G., personal
192 communication, 2008), lists the thickness recorded for each well in Mongolia. The
193 compilation process allowed us to estimate an average (of 5.1 m) for the 15 wells
194 registered in and around the W1 and W2 watersheds.

195 For estimations of each term in equation (1), two sets of automatic weather
196 stations (AWS), MG1 (45°49'11.30"N, 106°17'43.00"E) and MG2 (45°48'34.80"N,
197 106°16'51.40"E), were installed on 7 July 2008 and 3 May 2009, respectively, in order
198 to measure the basic meteorological and hydrologic variables (Fig. 1 and Table 1)

199 required for estimating evaporation and soil moisture storage. The MG1 station is
200 located within the *Caragana* community while the MG2 station is located on a surface
201 predominantly covered by *Allium*. An extensive and wide range of hydrologic
202 elements were also obtained. From the data, each term for (1) was derived directly or
203 estimated using an appropriate theory and methodology. Details are provided in the
204 Appendix. Briefly, the estimation/measurement schemes can be summarized as follows.
205 Precipitation, P , was derived from measurements obtained from the MG1 and IMH
206 stations. Estimates for evaporation, E , were made by applying the energy balance
207 method, using sensible heat flux estimated from the locally calibrated bulk equation.
208 Groundwater discharge, G_{out} , and surface runoff, R_{out} , from the watersheds were derived
209 using a combination of topographic surveys, groundwater level measurements, well
210 pumping tests, and information provided by local headsmen, while the amount of
211 groundwater extracted through the wells, U , was estimated based on animal numbers
212 and the daily unit of water consumption for each animal (Table 2 and Appendix).
213 Storage change, ΔS , within the watershed was estimated from groundwater level
214 observations and soil moisture measurements obtained from the AWSs by assuming that
215 these observations represented average conditions for the watersheds.

216

217 3. Results

218 Our observations and analyses are summarized in Figure 2 (seasonal changes
219 of water balance), Table 3 (annual water balance), Table 4 ($P - \Delta S$ and mean residence
220 time for different soil depth ranges), and Table 5 (the mean residence time \bar{t} for
221 shallow groundwater). A discussion of our results is found below.

222

223 3.1 The distribution of water at the surface: Where does precipitation go?

224 On an annual basis, the answer to the question above is quite clear - the
225 majority of precipitation, P , is lost to the atmosphere by evaporation, E . However, the
226 E/P ratio was found to greatly change both seasonally and annually. The other terms
227 of water balance were very small and may actually be neglected depending on the
228 purpose of the analysis.

229 During the three, one-year periods for which annual water balance was
230 estimated (Table 3), the annual precipitation value was 87.5-95.8 mm and corresponded
231 to 58-64% of long-term mean annual precipitation (150 mm) for Mandalgobi. As
232 mentioned in the Methods section, the observation period was characterized by weak
233 drought conditions. Seasonally, as can be seen from Fig. 2, inputs to the watershed
234 occurred as rainfall almost entirely during the warm season. Winter precipitation (i.e.,

235 snowfall) was minor and totals were 3.9, 6.3, and 8.0 mm for the 2008-2009, 2009-2010,
236 and 2010-2011 winter seasons, respectively.

237 In contrast to precipitation, evaporation took place not only during the warm
238 season but also during the winter season. For example, total evaporation at MG1 from
239 December 2008 through February 2009 was 14.1 mm. The result is somewhat
240 surprising since Mongolian winter is known by its severely cold climate, during which
241 one would expect little evaporation. However, the winter climate is also characterized
242 by continuously sunny weather and by a persistently cold Siberian air mass. As a
243 result, Penman's potential evaporation, PE , during the winter can be as large as 87.5 mm,
244 approximately 8% of annual PE .

245 As can be seen from Table 3, annual evaporation was 65.1-83.7 mm,
246 representing ~68-96% of precipitation during the same period. The value is close to
247 that reported by Yamanaka et al. (2007), obtained from measurements at four sites
248 surrounding the Mandalgobi area during the summer season from June through August.
249 However, our results indicate that this ratio changes markedly depending on the target
250 period. To understand the availability of energy and water for evaporation, these ratios
251 may also be compared with standard relationships such as the Budyko or Turc-Pike
252 functions and E/P and PE/P (e.g., Arora, 2002). Based on Table 3, the 3-year averages
253 can immediately be obtained as $E/P = 0.82$ and $PE/P = 11.6$. In a figure to show
254 functions with PE/P on the x -axis and E/P on the y -axis, the values are plotted within
255 the upper-right corner of the figure (e.g., Fig.1 of Aurora, 2002). General agreement
256 exists although $E/P = 0.82$ is located on the lower side expected for the high aridity
257 index of $PE/P = 11.6$.

258 Overall, annual water balance is dominated by precipitation and evaporation,
259 and to some extent by infiltration into the soil layer (see the discussion below on this
260 topic). As is clear from data provided in Table 3, groundwater discharge (G_{out}),
261 surface runoff (R_{out}), and groundwater use (U) are all minor components of water
262 balance within the two watersheds. It is likely that a small G_{out} and R_{out} would be
263 similar for other watersheds in the area, since the hydraulic gradient that determines G_{out}
264 and the surface gradient that determines R_{out} are expected to be small within this
265 generally flat terrain. With all water balance components either measured or estimated,
266 the water balance (1) should, in theory, be closed. However, in reality this is not the
267 case and the residual (i.e., the error term) is shown as ϵ in Table 3. On an annual basis,
268 this value is approximately in the range of -24 to 34 mm a^{-1} but is reduced to 3 to 4 mm
269 a^{-1} when the average of three years is considered, suggesting a random, rather than a
270 systematic, error for water balance estimations.

271

272 3.2 The role of soil moisture as a cushion for absorbing precipitation fluctuations

273 The soil column was found to play a major role in smoothing out fluctuating
274 precipitation inputs to each watershed. Such a result is essentially accomplished
275 because the soil column acts as a reservoir. When a drought period continues, soil
276 moisture is released for soil evaporation and transpiration and the growth and survival
277 of vegetation is maintained, while it is replenished during a rainy period. As a result,
278 the availability of water for vegetation fluctuates less than precipitation.

279 As mentioned above, on average, 82% of precipitation is lost by evaporation
280 each year. The remaining water, 12.7 mm a^{-1} (14% of P), goes to infiltration and
281 contributes to the storage change, ΔS . As can be seen in Fig. 2, on shorter time scales
282 this ratio is also quite variable, indicating seasonal variations for P and SWC and the
283 accumulated value of P and $P - \Delta S$. The value for ΔS in this case was determined based
284 on SWC data from AWSs located at the surface down to -1.3 m. As can be seen from
285 (1), the result should be the same as E under conditions of negligible G_{out} , R_{out} , U , and
286 ΔS within soils below the lowest levels. Thus, the general agreement found in Fig. 2
287 between the two provides partial verification for the evaporation estimates obtained by
288 (1).

289 As can be seen from the figure, P occurs intermittently while E and $P - \Delta S$ are
290 continuous, indicating a direct interaction between P and SWC during the wet period
291 and between E and SWC during the dry period. Also clear is that there are periods
292 where $\sum E > \sum P$. For example, beginning in February of 2011 through July of the
293 same year, accumulated evaporation continued to be larger than accumulated rainfall.
294 During these periods, evaporation consumes the stored soil moisture and drought
295 conditions can easily result. During the observation period, however, this type of
296 outcome did not occur for extended periods.

297 Some finer points in Fig. 2 also require clarification. First, during the winter
298 period, in contrast to the value of E obtained from the AWS, $\sum(P - \Delta S)$ did not
299 display an increase. The result is not surprising since TDR sensors are incapable of
300 detecting accurate soil moisture when the soil is frozen (see the Appendix for more
301 information). For this reason, the ΔS values estimated during cold seasons should be
302 treated with care. The second point to notice in Fig. 2 is two occasions of decrease for
303 $\sum(P - \Delta S)$. For the spring of 2010, as indicated by an increase in SWC and soil

304 temperatures above freezing, the decrease was due to the infiltration of melted snowfall.
305 Melted snowfall is not included in the calculation of P and thus resulted in a decrease
306 for $\sum(P-\Delta S)$. For spring 2009, however, the infiltration of melted snowfall had
307 already occurred by the end of March and cannot explain the decrease of $\sum(P-\Delta S)$.
308 One possible explanation for the underestimation of P is a tipping bucket rain gauge
309 with accumulated sands due to the dust storms that typically occur in the area during
310 March-April.

311

312 3.3 Soil water-groundwater interactions

313 We determined that the groundwater-soil moisture connection was very weak
314 during rainfall events and on rain-free days. As a result, groundwater recharge rarely
315 took place and only occurred during heavy rainfall events mainly in valley bottoms.
316 Groundwater is also not directly used by transpiration. Thus, the role of groundwater
317 in the hydrologic cycle is quite limited, as can be confirmed by the observational results
318 and the analyses explained below.

319 Table 4 lists the values of $P-\Delta S$ estimated for various depth ranges. The
320 list indicates which soil layers are the most actively involved in the annual hydrologic
321 cycle within the area. Clearly, the top soil layers play a major role. $P-\Delta S$ values
322 for the layer from 0-0.25 m are roughly 85-90% of those for the maximum depth range
323 of 0-1.3 m. Even those for the 0-0.075 layer accounted for some 70% and can also be
324 compared with the stable groundwater levels of GW1, GW2, and GW4 (Fig.2) that
325 usually do not respond to rainfall events (see the discussion below).

326 Table 4 also lists the mean residence time of soil water which was estimated by
327 assuming a steady state condition for each depth range. For the most active layers of
328 0-0.25 m, this is on the order of months, while for the range involving deeper layers it is
329 on the order of a year. Table 5 provides the mean residence time, \bar{t} , for shallow
330 groundwater as estimated from an analysis of the tritium concentration, C , of well
331 water samples taken on 12 May 2011 (see the Appendix for more details). The value of
332 \bar{t} was found to be in the range of 30-60 years. Due to a limited number of available
333 groundwater samples and the uncertainty involved in the choice of a piston-type flow
334 model, the residence time determined is, thus, not very accurate, but it is clearly much
335 longer than that of soil water, in agreement with results derived from the water balance
336 consideration outlined above. The larger picture here is that the shallow
337 groundwater-soil water connection is very weak to non-existent and periodic

338 connections in the form of groundwater recharge take place only rarely during heavy
339 rainfall events.

340 The arguments outlined above, based on mean residence time, can also be
341 supplemented by looking at the time-series data. For example, an apparent decrease in
342 groundwater levels due to evaporation was not observed (Fig.2), indicating a limited
343 connection between groundwater and soil water during sunny periods. The result is in
344 agreement with the findings of Satoh et al. (2012) who indicated, using stable isotope
345 analyses, that within the W1 and W2 watershed groundwater is not directly used for
346 transpiration.

347 During rainfall events, it is obvious that not all SWC values throughout the soil
348 column responded to all rainfall events. In general, only SWC values at shallower
349 depths responded, while those at deeper layers of 70-110 cm did not display an obvious
350 response. However, three cases were determined when all of the SWC values
351 increased, as follows: (i) at the end of April 2009, (ii) during the March-April period of
352 2010, and (iii) at the end of June 2011. The increase in SWC at the end of August
353 2008 may also be added to this category, although it is not quite clear if the change in
354 SWC at 70 cm and 110 cm were due to target rainfall events or to events that took place
355 earlier. Among them (including the questionable August 2008 case) only two cases
356 occurred in which an increase in groundwater level was also observed. One was for
357 the rainfall event on 29 August 2008 (total rainfall of 23.5 mm and a maximum
358 intensity of $0.7 \text{ mm } 10 \text{ min}^{-1}$) for which a small water level increase of GW2 was
359 observed. Another one occurred on 22 June 2011 (total rainfall of 18.5 mm and a
360 maximum intensity of $6.3 \text{ mm } 10 \text{ min}^{-1}$) when a GW4 water level increase was
361 observed. These events are, thus, rare occasions when groundwater recharge took
362 place. However, by comparing SWC and groundwater level changes, it is obvious that
363 the increases in groundwater level at GW2 and GW4 were more pulse-like than gradual
364 and took place much earlier than those of the deeper SWC at 70-110 cm where only
365 slow and gradual increases were observed. The result tends to support an argument
366 that infiltration and SWC increases on a hillslope are not directly connected to the
367 groundwater level increase observed within the valley bottom. Thus, groundwater
368 recharge is not uniform throughout the watershed but, rather, is a localized phenomenon.
369 This type of focused recharge also appears to be more common than distributed
370 recharge in the arid climate (e.g., Scanlon et al., 2006).

371 Heavy rainfall events and groundwater level increases could also have been
372 accompanied by surface runoff generation in valley bottoms. Although a direct
373 confirmation is not possible, interviews and an analysis of topographic surveys (see the

374 Appendix) indicate that such an assumption it is not inconceivable. According to our
375 analysis, surface runoff can be expected only once in a 2-3 year period and when
376 rainfall intensity exceeds 4-5 mm within a ten-minute period. For the 22 June event
377 mentioned above, this criterion was satisfied, as graphically shown in Fig. 2. The
378 rainfall intensity of the questionable 29 August event was, on the other hand, too small
379 to have caused surface runoff.

380

381 3.4 Groundwater recharge rates

382 The above argument tends to imply that the amount of groundwater recharge is
383 very small. Using available data, a crude estimation for the mean recharge rate, $\overline{q_z}$,
384 can be calculated using two approaches. For the first approach, (1) should be applied
385 for long-term mean values with $\Delta S = 0$ and $G_{out} = 0$, namely in the form of the following
386 equation:

387

$$388 \quad \overline{q_z} = \overline{P} - \overline{E} - \overline{R_{out}} \quad (2)$$

389

390 With a climatic mean of $\overline{P} = 150 \text{ mm a}^{-1}$ (for 1944–2011), an \overline{E} of 82% from \overline{P} ,
391 and the $\overline{R_{out}}$ obtained from Table 3, (2) leads to $\overline{q_z} = 27 \text{ mm a}^{-1}$.

392

In the second approach, $\overline{q_z}$ was determined from the mean residence time, \overline{t} ,
393 determined from the tritium concentration analysis and the storage of shallow
394 groundwater, \overline{S} , estimated from the mean thickness and the effective porosity of the
395 aquifer (see the Appendix for method details). The estimated value of $\overline{S} = 420 \text{ mm}$
396 for both the W1 and W2 watersheds and $\overline{t} = 28\text{-}59$ years yielded a $\overline{q_z}$ in the range
397 of 7-15 mm a^{-1} (Table 5). The values are on a lower side of those estimated by (2), but
398 on the same order of magnitude. Thus, the mean groundwater recharge rate in this
399 region appears to be on the order of 15 mm a^{-1} . Although for this region no additional
400 studies are available for comparing the calculated $\overline{q_z}$, the values are in the range of
401 reported groundwater recharge rates for arid and semiarid regions (e.g., Scanlon et al.,
402 2006), but on the higher side for annual precipitation, $\overline{P} = 150 \text{ mm}$.

403

404 4. Discussion

405 4.1 How much groundwater can be used for nomadic pastoralism?

406 The question above can be addressed by considering that shallow groundwater
407 withdrawal for nomadic pastoralism should not reduce groundwater resources over a
408 long time period. Thus, the maximum amount of groundwater use, U_{\max} , should be the
409 same as $\overline{q_z} - \overline{G_{out}}$; determined to be on the order of 15 mm a^{-1} , or 5.1×10^{-5} and $1.7 \times$
410 $10^{-4} \text{ km}^3 \text{ a}^{-1}$, or 1.4×10^5 and $4.6 \times 10^5 \text{ L d}^{-1}$ for watersheds W1 and W2, respectively.
411 The result can be compared with an actual water consumption of $9.0 \times 10^2 \text{ L d}^{-1}$ (W1)
412 and $3.0\text{-}3.7 \times 10^3 \text{ L d}^{-1}$ (W2), as determined from Table 2. Therefore, it is clear that
413 the level of U_{\max} is sufficient to allow the current level of nomadic pastoralism without
414 a reduction in groundwater resources within this region.

415 Interestingly, the U_{\max} values are on the same order of magnitude as those
416 preliminarily estimated for four watersheds within northeastern Mongolia where the
417 climate is more humid, has a larger mean annual \overline{P} of 200-250 mm, and a Mongolian
418 vegetation class of mountain forest steppe (Tsujimura, 2007). Since the amount of
419 water is judged to be sufficient for the two extreme vegetation classes, mountain
420 forest steppe and desert steppe, expected for nomadic pastoralism within steppe regions
421 of Mongolia, the result suggests that water is not a limiting factor, in general, for
422 nomadic pastoralism in Mongolia, at least for current climate conditions.

423 The above discussion provides a long-term mean and is useful for arguing a
424 case for short-term drought. Under a short-term drought, groundwater continues to be
425 used even though no groundwater recharge takes places. Thus, the question is how
426 long current groundwater storage can last in support of nomadic pastoralism. The
427 value can be estimated by deriving a S/U value. With available information for both S
428 and U in watersheds, S/U was determined to be on the order of 10^4 years. Therefore,
429 even during prolonged droughts, shallow groundwater resources are sufficient to
430 maintain current livestock numbers.

431

432 4.2 The past and future: Changes in animal numbers, climate, and well networks

433 The discussion provided above indicates that, at least at present, drinking water
434 from shallow groundwater is not a limiting factor for nomadic pastoralism. The
435 question to consider now is how factors have changed from the past and how they will
436 differ in the future based on current processes? By considering each factor, we
437 determined the crucial factor required for sustainable nomadic pastoralism in Mongolian
438 steppe. As explained below, the presence of a well network in Mongolian steppe that
439 guarantees access to shallow groundwater is the crucial factor.

440

441 *Animal numbers*

442 The present animal population in Mongolia is the largest it has ever been,
443 particularly since the introduction of a market-oriented economy in 1990-91. In 2007,
444 the total animal population in Mongolia was 40×10^6 , and can be compared with much
445 smaller and more stable numbers of 24×10^6 in the 1930s and 26×10^6 in 1990 (see
446 Fig.2 in Sugita et al, 2007). In Saintsagaan soum, a steady increase in livestock
447 number following the introduction of a market-oriented economy in 1990-91 was
448 observed (Fig. 3), with the exception of the 1999-2000 period when a nationwide ‘dzud’
449 (a disaster with damage and death to livestock caused by severe cold weather) took
450 place. Thus, in the past, the impact of grazing as compared to water balance should
451 have been even smaller. Considering possible impacts under assumed cases of
452 increased grazing pressure for the future is also possible. For these estimates, the U
453 value was determined for animal number increases that were 200%, 300% and 1000%
454 of current values. Our result indicated, however, that U remained a minor component
455 of (1), even with these dramatic increases. In reality, although the population of
456 livestock increased significantly after 1990-91, their numbers did not increase by more
457 than 100%.

458

459 *Climate*

460 The past climate can be estimated, to some extent, by looking into records for
461 historical precipitation, reconstructed based on tree-ring analyses. For example,
462 Pederson et al. (2001) provided a reconstructed precipitation record for the period from
463 1651-1995 for the northern portion of Mongolia, while Jacoby et al. (1999) provided
464 one for central Mongolia. Both studies indicate that there were no apparent continuous
465 trends of increase or decrease in precipitation. Pederson et al. (2001) also described
466 the presence of cyclic short-term wet and dry periods, with a standard deviation of 50.2
467 mm, and a significant peak in the power spectra at 10.8 and 12.8 years. Based on
468 instrument observations, the results were found to be similar to those obtained for the
469 recent period from 1942-1995. Thus, it is not unreasonable to assume that long-term
470 means and fluctuations of climate have remained approximately the same. Thus, the
471 statement that drinking water from shallow groundwater is not a limiting factor for
472 nomadic pastoralism in Mongolia can be extended to a longer time period. Such a
473 result is also in agreement with the study of Brutsaert and Sugita (2008) who found no
474 clear trend in long-term groundwater storage within the Kherlen River Basin (a target
475 area slightly different from the present study) in northeastern Mongolia from

476 1947-2006.

477 Larger uncertainties exist regarding future climates. However, projected future
478 climate studies are available. For example, using two dynamic downscaling schemes
479 in general circulation model outputs (based on the 'A2' scenario) using a regional
480 climate model, Sato et al. (2007) indicated a general decrease for precipitation on the
481 order of 20 mm during the July-August period for 2070s Mongolia as compared to
482 present. Since the present recharge rate is very small anyway, the level of decrease
483 should likely only have a minor impact on groundwater. However, for vegetation
484 growth, this change could have a strong impact and is, therefore, discussed below.

485

486 *Well network*

487 Another factor that must be considered for the past and future is the presence of
488 wells. As mentioned above, when livestock migrates with herders, both periodically and
489 seasonally (e.g., Cribb, 1991), seeking a continuous supply of water and a pasture for
490 grazing, the main water source is shallow groundwater. For water to be available, the
491 widespread access to shallow groundwater via the presence of wells is required.
492 Without shallow wells animals have no way to make use of water. They also cannot
493 migrate even if sufficient water is available within a shallow aquifer.

494 In Mongolia, the well network in remote pasturelands appears to have begun
495 during the era of Ugedei Khan (1206-27), who ordered wells to be dug to supply water;
496 listed as one of the four deeds in Mongolian history (Anonymous, 1982; Baranchuluun
497 et al., 2004). Although it is not clear how widespread the initial construction of wells
498 was in the past, Sharkhuu (1975) provides a hint in archived records regarding the
499 various disputes amongst people living in the Qing Dynasty (1616-1912) which
500 extended its territory into present-day Mongolia. Amongst the archived records are
501 conflicts regarding the use of wells. Thus, from these descriptions, it appears that at
502 least in the Qing Dynasty era the presence and use of wells in pasturelands were already
503 common. Such wells continue to exist and were maintained until recently through a
504 social institution called 'neg nutgiinhan' before the 1930s (Chuluun and Ojima, 2002)
505 and a pastoral cooperatives system known as 'negdel' since the late 1950s.

506 Following introduction of the market-oriented economy in 1990-91 in
507 Mongolia, 'negdel' was privatized and the maintenance function of the wells was
508 abandoned or weakened. As a result, in 2000 the nationwide number of wells in
509 pasturelands decreased to 57% of that found in 1990 (Fig.3). Since 2000, a decrease in
510 well decline slowed and an increase was reported. The exact reason(s) for the increase
511 is(are) not clear, although the repair and/or construction of wells offered as

512 compensation for damage made to pasture lands by Mongolia's booming mining
513 industry and the introduction of national plans such as the National Livestock Program
514 (approved in 2010 to invest more funds in the livestock sector) may be related. Still,
515 the future of the well network is not yet uncertain and could be a major problem in
516 Mongolia since there is no clear policy for maintaining the well network in rural
517 rangelands.

518

519 4.3 Feed supply (vegetation) as a limiting factor for nomadic pastoralism

520 The discussion above indicates that drinking water supplied from shallow
521 groundwater has been and will likely not be a limiting factor for nomadic pastoralism as
522 long as well networks exist and are maintained. Even if one well dries up, it is
523 possible to move to other areas with a smaller grazing pressure containing a water
524 supply. But does such knowledge imply that increased grazing far above current
525 levels is acceptable and sustainable? In reality, an increase in grazing pressure by
526 200% is likely not sustainable, not because of the impact on the water balance as has
527 been shown above, but due to a lack of sufficient vegetation to feed the animals. Such
528 a lack of vegetation would result for at least two reasons, as discussed below.

529

530 *Overgrazing and desertification*

531 A loss of vegetation under heavier grazing will likely result from an increase in
532 animal numbers. For example, Chen et al. (2007) indicated by way of a numerical
533 simulation employing a process-oriented carbon cycle model that both above-ground
534 biomass (AB) and net primary production should keep decreasing and should eventually
535 result in a permanent loss for vegetation if a grazing pressure of $S_r > 0.7 \text{ SEU ha}^{-1}$
536 continues over a long time period within the steppe areas of northeastern Mongolia that
537 currently have an annual precipitation rate of 187 mm and a mean S_r of 0.7 SEU ha^{-1} .
538 Thus, the current level of grazing represents the maximum the area can support in a
539 sustainable manner. For the study basins examined, the S_r is 0.56 SEU ha^{-1} , as
540 mentioned above. Since our study areas are located in a drier region than those studied
541 by Chen et al. (2007), the maximum sustainable S_r is expected to be even smaller.
542 Therefore, an increase in the grazing pressure over a much larger level than the current
543 S_r would likely result in the long-term degradation of vegetation.

544

545 *Water and vegetation*

546 Another potential cause for a loss of vegetation, making it difficult to feed
547 animals, comes from prolonged clear days without significant rainfall events, as was the

548 case in 2011 (Fig. 2). Actually, this type of temporal loss for fresh AB takes place
549 quite frequently because vegetation, particularly herbaceous plants, respond quickly (on
550 daily basis) to water stresses that easily result in the withering of leaves or dormant
551 conditions under continued dry periods. A detailed isotopic study by Satoh et al.
552 (2012) within the W1 watershed indicated such a mechanism. The root systems of
553 herbaceous plants only extend down to 20 cm, so they take water from soils within the
554 upper 20 cm layer. Since this top soil layer dries out very quickly with soil
555 evaporation under rain-free conditions (Fig.2), herbaceous plants are susceptible to
556 water shortages. However, dormant conditions for vegetation without AB can easily
557 be recovered with sufficient rainfall amounts. For example, Satoh et al. (2012) have
558 reported a case in which the re-emergence of AB for herbaceous plants following one
559 month of rainfall absence was observed only two days subsequent to a rainfall event of
560 6.4 mm and that surface SWC increased from 3 to 5%. Then, following a one week
561 dry period, SWC dropped again to the 3-4% level and a withering of leaves was
562 observed. However, a total of 6.3 mm rainfall for two continuous days brought SWC
563 up to 9% and the re-growth of AB resulted. Such plant behavior can also be
564 understood from a hydrologic view point using the information listed in Table 4 in
565 which the mean residence time was 1 to 2 months and the mean water storage was only
566 on the order of 10 mm within the upper soil layers from which herbaceous plants take-in
567 water. Thus, it is quite natural that water shortages and recovery processes take place
568 within a relatively short period of time.

569 All of these arguments and discussions illustrate that much before the shortage
570 of water, feed to livestock itself becomes a problem. Water shortage to vegetation and
571 the resulting loss of pasture will likely emerge as a limiting factor for continuous
572 nomadic pastoralism. Such drought conditions, however, are often limited to certain
573 areas, so nomads can migrate to other areas to seek better pasture conditions as long as
574 the drought is not widespread or the animal number is not too large such that sufficient
575 space is left for migration within the surrounding areas under better conditions.
576 However, for migration to be successful, a well network is necessary so that nomads
577 can move to better areas that contain not only pasture but water supplies from shallow
578 groundwater. Again, the importance of the well network should be stressed.

579

580 5. Concluding Remarks

581 In the present study, the main limiting factors for nomadic pastoralism in
582 Mongolian steppe were investigated by determining water balance and hydrologic
583 processes in two watersheds located in central Mongolia. Since water is often

584 considered to be a limiting factor, a focus was directed towards water availability. In
585 terms of drinking water from shallow groundwater, it was determined that sufficient
586 water exists for consumption by livestock. Such was the case in all seasons throughout
587 a year within the target area, in the past, and, possibly, for the future. Also, based on a
588 comparison with similar studies conducted elsewhere in Mongolia, the results presented
589 are likely applicable to larger areas of Mongolian steppe.

590 Although shallow groundwater is sufficient, water is more likely to be a
591 limiting factor for the continuation of nomadic pastoralism due to two issues. The first
592 issue is the decline of the well network. As indicated above, the number of wells
593 decreased following introduction of the market-oriented economy in 1990-91, and the
594 maintenance function of wells in Mongolia was weakened. Thus, although shallow
595 groundwater is sufficient, there is a possibility that access to water could be a problem.
596 The second issue to consider is the water-vegetation relationship. For this issue,
597 periods without rainfall result in the temporal loss of aboveground biomass for
598 herbaceous plants that are the main livestock feed source. When a loss of
599 aboveground biomass occurs, a solution that has continued over centuries is simply to
600 migrate to a better area where pasture is abundant due to recent rainfall events. Such is
601 acceptable if the drought condition is not extended to a larger area, and if a well
602 network exists such that nomads can make use of them in order to feed livestock. In
603 this sense, water is an indirect limiting factor for nomadic pastoralism in Mongolian
604 steppe. Interestingly, a study based on a large scale survey of herders by Sternberg
605 (2008) also identified water resources and pasture quality as two of their paramount
606 concerns.

607 The conclusions presented above were derived based on the first part of our
608 study, namely, water balance estimations over three years in two watersheds in central
609 Mongolia, which can be summarized as follows. The majority (82%) of annual
610 precipitation, P , is lost to evaporation (E), 14% is allotted to soil storage changes (ΔS),
611 and the rest, a small proportion, travels in surface and groundwater runoff. On shorter
612 time scales, the E/P ratio changes greatly and can be $>100\%$. Variation of the E/P
613 ratio is reflected in and absorbed by the change in soil moisture storage, but not that of
614 groundwater in most cases because only the top soil layers are involved in the active
615 hydrologic cycle. Indeed, the residence time of groundwater is much longer (26-55
616 years) than that of soil water (36-145 days). Thus, recharge to shallow groundwater
617 takes place only for heavy rainfall events within the valley bottom, likely with the
618 occurrence of ephemeral surface runoff. As a result, the soil water-groundwater
619 connection is very weak. Estimated groundwater storage within the shallow aquifer is

620 $S = 420$ mm. The amount of the annual withdrawal of shallow groundwater from
621 wells for daily use by livestock is as small as $<0.1\%$ of annual precipitation (P),
622 87.5-95.8 mm.

623 On a final note, it should be mentioned that, given the remote target area with
624 severe environmental conditions, water balance estimates in the present study are not
625 without uncertainties. Thus, interpretations based on the water balance analysis should
626 also naturally involve uncertainties. Nevertheless, in this study the problem was
627 remedied to some extent by employing multiple approaches in which the water balance
628 components were estimated using two independent methods whenever possible.
629 Although the supplementary information and the results naturally also contain certain
630 errors, all of the available information was consistent and was used to validate the
631 results obtained in the analysis. Another issue that deserves to be mentioned is the
632 representativeness of our detailed study for the two watersheds. As mentioned, the
633 watersheds are located near Mandalgobi and have a mean stocking rate somewhat larger
634 than the average for the larger 'aimag' area, likely due to the closeness of the city.
635 Since a wide variety of conditions exist within the Mongolian steppe region, performing
636 a large-scale survey for validating and supplementing the results presented here is
637 desirable.

638

639 Acknowledgement

640

641 We thank I. Kaihotsu (Horishima U.) and the Japan Aerospace Exploration Agency for
642 providing wind speed data from their AWS, and G. Davaa and D. Oyunbaatar (Research
643 and Information Institute of Meteorology, Hydrology, and Environment (IMH)) for
644 facilitating local logistics and for arranging the maintenance of stations throughout the
645 Meteorological Centers of IMH at Mandalgobi and Dalanzadgado. We are also
646 grateful to T. Satoh and Y. Morinaga (U. Tsukuba) for participating in the field
647 observations for this study, and to Y. Konagaya (National Museum of Ethnology of
648 Japan), S. Mori (IMG, Inc.), and G.U. Nachinshonhor (Okayama U.) for providing us
649 with references on the history of well construction in Mongolia, and for an anonymous
650 referee and associate editor for providing valuable comments to improve the quality of
651 the manuscript. Finally, we also express appreciation to N. Fujita and N. Yamamura
652 (Research Institute for Humanity and Nature (RIHN)). Without their initiatives and
653 leadership the experiments for this study would not have been possible. Our research
654 was supported and financed, in part, by the RIHN project "Collapse and Restoration of
655 Ecosystem Networks with Human Activity" and by a Grant-In-Aid for Scientific

656 Research (A, no.24241053) from the Japan Society for the Promotion of Science.

657

658 Appendix

659 Details of the method employed for water balance estimations

660 *Watershed boundaries*

661 Watershed boundaries were determined using a map and GPS surveys. For
662 the surveys, a topographic map of 1:100,000 and a map (Fig.1) created using 90-m
663 digital elevation data from the NASA Shuttle Radar Topographic Mission (SRTM)
664 (CGIAR-CSI, 2008) were employed. The divides determined on these maps by GIS
665 were verified and corrected wherever necessary by in-situ surveys using a GPS receiver.
666 The watershed areas for W1 and W2 were determined to be $A = 3.3967 \text{ km}^2$ and $A =$
667 11.3567 km^2 , respectively.

668

669 *Soil moisture*

670 For soil water content (SWC) measurements, TDR (time domain reflectometry)
671 sensors, inter-calibrated prior to installation and installed at the MG1 and MG2 stations,
672 were employed and outputs were corrected based on soil temperature data in order to
673 minimize temperature influences (see Yamanaka et al., 2003). Note that although the
674 SWC measurements were continuous, the SWC measurements obtained during the
675 winter were not as reliable as those obtained during summer because TDR sensors are
676 incapable of detecting accurate soil moisture when they are frozen (e.g., Yoshikawa and
677 Overduin, 2005; Kahimba and Sri Ranjan, 2007; Watanabe and Wake, 2009).

678

679 *Assumptions in water balance estimations*

680 As mentioned in the methods section, for application of the water balance
681 equation (1) we assumed that the shallow aquifer is underlain by an impermeable layer
682 and that no leakage occurs. Based on the steady groundwater level, the assumption
683 was judged to be acceptable. However, there is a possibility that the excessive
684 withdraw of deep groundwater may induce the leakage of shallow groundwater down to
685 deeper aquifers (e.g., Rathod and Rushton, 1991; Yamanaka et al., 2011). Such could be
686 the case in Mandalgobi since municipal water for the city comes from three wells
687 located some 30 km from the city and three wells within the city (Tuinhof and Nemer,
688 2009) with depths of 160 m (Tsogtbaatar and Janchivdorj, 2009). Perhaps the amount of
689 extracted water ($10^3 \text{ m}^3/\text{day}$ during winter and $7.5 \times 10^2 \text{ m}^3/\text{day}$ during summer (Tuinhof
690 and Nemer, 2009)) is not large enough to cause large-scale induced seepage.

691

692 *Precipitation*

693 As mentioned, P was determined from AWS measurements. However, the
 694 tipping bucket rain gauge at MG1 was not capable of measuring snowfall during the
 695 winter. Thus, to supplement AWS measurements, daily precipitation data measured
 696 manually at the IMH station were also used for considering the water balance of each
 697 watershed.

698

699 *Evaporation*

700 Evaporation, E , was estimated from the following energy balance equation:

701

$$702 \quad R_n - G = H + LE \quad (A.1)$$

703

704 where R_n is net radiation, G is the soil heat flux, $LE (= L_e \times E)$ is the latent heat flux, and
 705 L_e is the latent heat for vaporization. H is the sensible heat flux and was estimated by
 706 applying the following bulk equation for sensible heat flux:

707

$$708 \quad H = \frac{ku_*\rho c_p(T_s - T)}{\ln\left(\frac{z-d_0}{z_{0h}}\right) - \Psi_h\left(\frac{z-d_0}{L}\right)} \quad (A.2)$$

709

710 where k is Karman's constant; u_* is the friction velocity; ρ is the air density; c_p is the
 711 specific heat of air at constant pressure; T_s and T are the surface and air temperature,
 712 respectively; z is the height of the T measurement; and d_0 is the displacement height,
 713 assumed to be 2/3 of the mean vegetation height (= 0.145 m for *Caragana*) for MG1
 714 and zero for MG2. The symbol z_{0h} represents scalar roughness for sensible heat, Ψ_h
 715 is the stability correction function for sensible heat, and L is the Obukhov length. The
 716 frictional velocity, u_* , was derived by the bulk equation for momentum flux, as follows:

717

$$718 \quad u_* = \frac{ku}{\ln\left(\frac{z-d_0}{z_0}\right) - \Psi_m\left(\frac{z-d_0}{L}\right)} \quad (A.3)$$

719

720 where u is the wind speed, z_0 is the roughness length, and Ψ_m is the stability correction
 721 function for momentum.

722

723 Surface parameters for z_0 and z_{0h} were first determined from (A.2)-(A.3) using
 fluxes for H , LE , and u_* obtained from an eddy correlation approach. More specifically,

724 the method of Toda and Sugita (2003) was applied to the data, in which the left hand
725 side (LHS) (i.e., the measured fluxes) and the right hand side (RHS) of (A.2)-(A.3) (i.e.,
726 the estimated fluxes) for a given value of z_0 and z_{0h} were compared. The process was
727 repeated by changing z_0 and z_{0h} over a small interval, and parameters that yielded the
728 smallest rms error were selected. For the present analysis, rms error, the statistics of
729 R^2 , the ratio of the means for LHS and RHS, and the regression constants of a and b in
730 $\hat{y} = ax + b$ (where \hat{y} is the measured flux and x is the estimated flux) were considered.

731 To apply this approach, intensive observations were performed during the
732 summer of 2009; and an eddy correlation system with a sonic anemometer (Gill
733 Instruments, Ltd., R3-50) and an open-path gas analyzer (LI-COR Inc., LI-7500) was
734 added to the AWS system from 23-28 July at MG1 and from 28-30 July at MG2 in
735 order to determine the surface roughness parameters of the area so that the bulk
736 approach for estimating surface fluxes could be applied (see below).

737 Based on observation results, $z_0 = 1.73 \times 10^{-3}$ m, and $z_{0h} = 1.71 \times 10^{-5}$ m were
738 determined for the area surrounding the MG1 station. The values agree with the
739 theoretical estimates for bluff-rough surfaces (e.g., Fig. 4.24 of Brutsaert (1982)), more
740 so than those for a surface covered with permeable roughnesses. The finding is not
741 surprising since the average fractional coverage of *Caragana* was only 3-4% (Satoh et
742 al., 2012) and the surface is closer to that of bare soil than a vegetated surface. The
743 same values of z_0 and z_{0h} were used for the entire year and for MG2 following
744 verification that the values produced fluxes that agreed, on average, with measured
745 fluxes during the intensive observation period.

746 The soil heat flux, G , was estimated as a fraction of R_n . Constants (0.68 for
747 daytime and 1.1 for nighttime) were determined based on measured values for H and LE
748 obtained from the eddy correlation approach and R_n from net radiometer data obtained
749 during intensive measurements. G values were estimated as the residual term of the
750 energy balance equation from $G = R_n - LE - H$. Although it is possible to use the G
751 obtained from a soil heat flux plate, this approach was rejected based on a preliminary
752 analysis in which closure of the energy balance (A.1) in the form of $y = ax + b$ and the
753 ratio of the means \bar{y}/\bar{x} in which $x = R_n - G$ and $y = H + LE$ (e.g., Wilson et al., 2002)
754 was evaluated. The result was $a = 0.43$, $b = -50$, and $\bar{y}/\bar{x} = 0.42$ and clearly
755 indicated the presence of a larger imbalance in the energy balance than the values
756 reported in the literature. Following a careful check of each term, we suspected that
757 the soil heat flux, G , measured by the soil heat flux plate was not representative of the
758 area and resulted in underestimations that caused an imbalance in the energy balance.
759 Due to this finding, we decided not to use the measured G .

760 With measurements and parameters, it is possible to continuously estimate
761 fluxes from 30-min averaged AWS measurements. However, for the period from
762 April through July of 2009 we encountered a problem with the wind speed sensor at
763 MG1. Due to the malfunction, wind speed values during this period were estimated
764 from hourly wind speed measurements obtained from a nearby AWS operated by the
765 Univ. Hiroshima. For estimations, a conversion equation was derived based on
766 measurements obtained when both AWSs were operating simultaneously.

767 Since (A.1)-(A.3) are implicit, an iteration procedure was applied in order to
768 derive the fluxes of H , u_* , and LE . Thus, $L = \infty$ was assumed for deriving the first
769 estimate for H and u_* , and LE from (A.1). The procedure produced the first estimates
770 for L and allowed determinations of Ψ_m , Ψ_h , and a second round of estimates for H ,
771 u_* , and LE , etc. The procedure was repeated until fluxes sufficiently converged. The
772 derived fluxes for MG1 and MG2 were found to be quite similar. Therefore, we decided
773 to use the fluxes obtained for the MG1 stations for additional calculations for both
774 watersheds in what follows. This has an advantage for having evaporation over longer
775 time periods.

776

777 *Groundwater level*

778 The water table level of the three wells, GW1, GW2, and GW4, was manually
779 measured and recorded daily by local herders. Manual recording was chosen due to
780 the difficulty in recovering automatic sensors in remote areas, especially after a full year.
781 Manual water level data were quality checked in order to screen (and correct when
782 possible) suspicious data. An example of a typical correction occurred due to shifts in
783 water level prior to and following the winter season because during the winter well
784 water was frozen and no measurements were performed. We also followed-up on
785 manual reports when we suspected that the reference for ground level was somehow
786 moved and caused a shift in the water level. An additional example of data correction
787 occurred due to unrealistic fluctuations for water levels reported during the first year.
788 We corrected first year data during the second year after issuing instructions for more
789 careful measurements.

790

791 *Groundwater discharge*

792 For the W1 watershed, groundwater discharge can be assumed to be zero
793 because GW1 is located at the center of a local depression near the watershed boundary.
794 From this depression there is no apparent outlet towards the downstream direction.

795 For the W2 watershed, estimates of G_{out} were obtained by applying Darcy's law,

796 as follows:

797

$$798 \quad G_{out} = q_x \frac{A_c}{A} = -k_h \frac{dh}{dl} \frac{A_c}{A} \cong -k_h \frac{h_2 - h_1}{l_{2-1}} \frac{A_c}{A} \quad (\text{A.4})$$

799

800 where A_c is the cross-sectional area of groundwater discharge from a watershed of area
801 A , q_x is the specific groundwater flux, k_h is the hydraulic conductivity, and dh/dl is the
802 hydraulic gradient. The value of dh/dl was estimated from the difference for the
803 hydraulic head of observational wells GW2 and GW4 located along the direction of the
804 main discharge direction as implied by surface topography over a horizontal distance of
805 l_{2-1} .

806 The value of k_h was determined by applying the Theis well recovery test (e.g.,
807 Kruseman and de Ridder, 1990) to wells GW1 and GW4. All water within the wells
808 was first emptied, then water recovery was recorded in order to estimate transmissivity,
809 then k_h for an aquifer with a known thickness in and around the W1 and W2 watersheds
810 was determined. From tests performed from 25-31 July 2009 at GW1 and 28 July at
811 GW4, values of $k_h = 2.1 \times 10^{-8} \text{ m s}^{-1}$ for GW1 and $k_h = 2.7 \times 10^{-7} \text{ m s}^{-1}$ for GW4 were
812 obtained. The obtained k_h values are in the general range of those expected for an
813 aquifer with unconsolidated materials of silty sand or silt (e.g., Freeze and Cherry,
814 1979). For estimations of G_{out} for the W2 watershed, the k_h value was determined
815 based on the adopted GW4 well recovery test. Cross-sectional area was determined
816 from a GPS survey and from information on the thickness of the aquifer as well as the
817 mean water table depth.

818

819 *Surface runoff*

820 Surface runoff, R_{out} , can be assumed to be zero for the W1 watershed for the
821 same reason that $G_{out} = 0$ and because no gully formation was found within the local
822 topography of the watershed outlet. In contrast, there was a clear indication of surface
823 runoff within the topography of the W2 outlet. Therefore, R_{out} was estimated based on
824 the following consideration. Interviews with the local population allowed us to obtain
825 crude estimations for the frequency and magnitude of surface runoff occurrences.
826 From interviews we learned that W2 surface runoff at the outlet of the catchment (i.e., at
827 around GW2) had been observed only once every 2-3 years and that when it occurred it
828 had a depth of several centimeters and lasted, at most, several hours. We then
829 compared the report of locals with AWS rainfall data. Over approximately three
830 summer seasons the largest recorded rainfall events had an intensity of 4.8 and 6.3 mm

831 within a ten minute period. A rainfall intensity of $>2.5 \text{ mm } 10 \text{ min}^{-1}$ occurred five
832 times during the same interval. Thus, a value of $\sim 4\text{-}5 \text{ mm } 10 \text{ min}^{-1}$ could likely be
833 adopted as a threshold value above which overland flows result. Interestingly, Onda et
834 al. (2007) reported, based on observations for two years in two hilly watersheds located
835 in northeastern Mongolia, that a threshold value of $4 \text{ mm } 10 \text{ min}^{-1}$ initiated surface
836 runoff. Note that rainfall events with an intensity of 4.8 and $6.3 \text{ mm } 10 \text{ min}^{-1}$ took
837 place on days with daily rainfall totals of 10.0 and 18.5 mm, respectively, that have a
838 return period of 0.9 and 1.7 years, respectively, as determined from annual maximum
839 daily rainfall amounts from the IMH station over 65 years fitted using the Weibull
840 plotting position formula (e.g., Brutsaert, 2005). Similarly, the 2-year and 3-year
841 rainfall values were, respectively, 21 and 27 mm day^{-1} .

842 The maximum depth (within the stream cross-section) of surface runoff and the
843 duration of runoff were assumed to have values of 2 cm, 5 cm, and 10 cm, and 1 to 3
844 hours to examine their sensitivity to water balance. However, the use of different
845 depths and duration did not produce significantly different results.

846 The mean velocity for surface runoff was estimated by applying the
847 Gauckler-Manning equation (e.g., Brutsaert, 2005). Based on visual observations, the
848 roughness parameter $n = 0.022$ was used for a straight channel with a sandy river bed.
849 The mean channel gradient (0.016) and the cross sectional shape of 11 points along the
850 channel from the beginning of the gully toward the downstream over a distance of 0.925
851 km were determined from the in-situ survey. The mean hydraulic radius and the
852 cross-sectional area of flow were then determined from the wetted areas of the 11 cross
853 sections for the assumed depths. The values are 6.3 cm and 0.36 m^2 , respectively, for
854 the assumed 10-cm depth.

855

856 *Water withdrawal from wells by local herdsman*

857 Water withdrawal by local herdsman was estimated for the current animal
858 numbers (Table 2) obtained from annual official statistics in 2007 (as compiled by the
859 National Statistical Office), from information provided by local herdsman in 2009, and
860 from unit water consumption values for which several sources were available. For
861 example, Baranchuluun et al. (2004) listed water use values for different seasons and/or
862 for the different life stages of livestock. The Minister of Nature and Environment
863 (1995) also provides standard water consumption values for the summer and winter
864 seasons. Although there are some differences in the listed values in these references,
865 for our purpose of estimating annual U values, the mean annual unit consumption of
866 water for each livestock type was derived and used for the analysis (Table 2).

867

868 *Groundwater Storage*

869 Groundwater storage, S , was estimated based on the thickness and effective porosity of
870 the aquifer. The effective porosity value was assumed to be the same as the mean
871 specific yield (0.3) of 163 wells (depth <40 m) in Saintsagaan soum. The result
872 appears to be on the higher side for an aquifer of sandy to silty materials. The mean
873 thickness of the aquifer was first determined by assuming that the aquifer thickness for
874 the location of the wells was 5.1 m, the average aquifer thickness for 15 wells registered
875 in and around the W1 and W2 watersheds in the Well Database. We also assumed that
876 thickness decreases linearly along the topographic slope from the valley bottom toward
877 the watershed boundary (the topographic divide) where the thickness was assumed as
878 zero. More specifically, aquifer depth was first determined manually at approximately
879 20 points within the W1 and W2 watersheds along the slope. The Kriging interpolation
880 was then applied together with zero thickness information on the divide in order to
881 determine the distribution for thickness within the watershed. The mean aquifer depth of
882 each watershed was determined to be 1.4 m for W1 and 1.3 m for W2, which, in turn,
883 produced the amount of storage for each watershed.

884

885 *Storage change*

886 In theory, it should be possible to derive storage change from the measured water
887 levels of the observation wells and soil moisture profile measurements by assuming that
888 they represent the entire basin. However, as mentioned above, well water level data as
889 measured manually by local herders were judged not to be as accurate for determining
890 water level changes as had been hoped. However, what these data did indicate was
891 that water levels were very stable without a clear seasonal trend and that response to
892 rainfall events and daily water withdrawals, in most cases, were not pronounced. Thus,
893 assuming that the storage change in groundwater is usually negligible is a reasonable
894 assumption. For the storage change within soil water, SWC values measured at the
895 MG1 and MG2 stations were used for estimating ΔS from the surface down to -1.3 m.
896 Since the average water table depth in this area is 2.1 m (as obtained from the Well
897 Database of Mongolia) and since the SWC value did not change much at -1.1 m (see the
898 Results section), ΔS determined this manner should provide acceptable estimates for
899 storage changes within the soil layer.

900

901 *Residence time of groundwater*

902 If one can assume piston flow for groundwater, the mean residence time, \bar{t} , of

903 shallow groundwater and the tritium concentration, C , are related by the following
904 equation (e.g., Ozyurt and Bayari, 2005):

905

$$906 \quad C = C_0 \exp(-\bar{t}/T) \quad (\text{A.5}).$$

907 where C_0 is the tritium concentration at the time of groundwater recharge and T is the
908 average lifetime of tritium (≈ 17.8 years). The value of C_0 can be estimated using the
909 past record of tritium concentration data for rainfall in the region and the radioactive
910 decay of tritium. The former time series data were constructed in Higuchi (2005)
911 using data obtained in Ulaanbaatar in Mongolia (1990-2000), Havarovsk in Russia
912 (1970-1983), and Ottawa in Canada (1970). Values for C_0 were visually estimated
913 from Fig. A1 as 80-200 TU for GW1 and 50-100 TU for GW2 and GW4, from which
914 the mean residence time, \bar{t} , of shallow groundwater was estimated (Fig. A1 and Table
915 5).

916

917 Reference

- 918 Anonymous, 1982. *The Secret History of the Mongols Vol. 1* (translated by Cleaves, F.
919 W.), Harvard Univ. Press, Cambridge, 277p.
- 920 Arora, V.K. 2002. The use of the aridity index to assess climate change effect on
921 annual runoff. *J. Hydrol.*, 265:164-177
- 922 Baranchuluun, Sh., Chanlmanii, L., Lugarmaa, M., 2004. *Water Supply in Pasturelands*
923 (Баранчулуун, Ш., Чандмань, Д. and Дугармаа М. (2004), Бэлчээр усжуулалт, ,
924 Дархан-Сэлэнгэ ХХК, 183p.) in Mongol.
- 925 Brutsaert, W., 1982. *Evaporation into the Atmosphere: Theory, History, and*
926 *Application*, D. Reidel Pub. Co., 299p.
- 927 Brutsaert, W., 2005, *Hydrology: An Introduction*, Cambridge Univ. Press, 605p.
- 928 Brutsaert, W., Sugita, M. 2008. Is Mongolia's groundwater increasing or decreasing?
929 The case of the Kherlen River basin. *Hydrol. Sci. J.*, 53, 1221-1229. doi:
930 10.1623/hysj.53.6.1221
- 931 Byambakhuu, I., Sugita, M., Matsushima, D., 2010. Spectral unmixing model to assess
932 land cover fractions in Mongolian steppe regions. *Remote Sens. Environ.*, 114,
933 2361-2372 doi:10.1016/j.rse.2010.05.013.
- 934 Chen, Y., Lee, G. Lee P., Oikawa, T., 2007. Model analysis of grazing effect on
935 above-ground biomass and above-ground net primary production of a Mongolian
936 grassland ecosystem. *J. Hydrol.*, 333, 155-164, doi:10.1016/j.jhydrol.2006.07.019.
- 937 CGIAR-CSI, 2008. *SRTM 90 m Digital Elevation Data*,

- 938 <http://srtm.csi.cgiar.org/Index.asp>. Accessed 12 April 2009
- 939 Chuluun T., Ojima D., 2002. Sustainability of pastoral systems in Mongolia, in
940 *Fundamental Issues Affecting Sustainability of the Mongolian Steppe*, ed. by
941 Chuluun, T. and Ojima, D., Interpress, Ulaanbaatar, 52-57.
- 942 Cribb, R., 1991. *Nomads in Archaeology*, Cambridge Univ. Press, 253p.
- 943 Dorzhgotov, D., 2003. *Soils of Mongolia*. Admon, Ulaanbaatar, 287p. (in Mongol).
- 944 Freeze, R.A., Cherry, J.A., 1979. *Groundwater*. Prentice-Hall, 604p.
- 945 Healy, R.W. 2010. *Estimating Groundwater Recharge*. Cambridge Univ. Press. 256p.
- 946 Higuchi S. 2005. *Groundwater Flow System Study Revealed by Environmental*
947 *Tritium and 3-D Groundwater Simulation in Kherlen River Basin, Mongolia*, MS
948 Thesis, Graduate school of Science and Technology, Kumamoto University, 89p.
949 (in Japanese).
- 950 Jacoby, G. C., D'Arrigo, R. D., Pederson, N., Buckley, B. M., Dugarjav, Ch., Mijiddorj,
951 R., 1999. Temperature and precipitation in Mongolia based on dendroclimatic
952 investigations, *IWA J*, 20, 339-350.
- 953 Kahimba, F.C., Sri Ranjan, R., 2007. Soil temperature correction of field TDR readings
954 obtained under near freezing conditions, *Can. Biosys. Eng.*, 49, 1.19-1.26.
- 955 Kruseman, G.P., de Ridder, N.A., 1990. Analysis and Evaluation of Pumping Test Data,
956 Revised Edition, International Institute for Land Reclamation and Improvement,
957 Publ. 46, 377p.
- 958 Matsubara, M., 2005. Introduction: toward the compilation of Eurasian history, in
959 Matsubara, M., Konagaya, Y., and Yang, H. ed., 2005. *Message from Eurasian*
960 *Grasslands*, Heibonsha, Ltd., Tokyo, 11-29.
- 961 Mineral Resources Authority of Mongolia and Mongolian Academy of Sciences, 1998.
962 *Geological Map of Mongolia, Scale 1:1,000,000*, Ulaanbaatar, available on line at
963 Mongolian Mining Registry and Cadastre System (URL:
964 http://www3.gaf.de/Mongolia_mining/pages/pub/downloads.html)
- 965 Mineral Resources Authority of Mongolia, 2001. *Distribution of Deposits and*
966 *Occurrences in Mongolia (at the scale of 1:1,000,000)*, Ulaanbaatar, available on
967 line at Mongolian Mining Registry and Cadastre System (URL:
968 http://www3.gaf.de/mongolia_mining/pages/pub/downloads.html)
- 969 Minister of Nature and Environment, 1995. *Water Use Statistics by Temporal*
970 *Regulation (Norm or Standard)*, Ministry of Nature and Environment, Order No.
971 153, 153p.
- 972 Miyawaki, J., 2002. *History of Mongolia*, Tosui Shobo, Tokyo, 295p. (in Japanese).
- 973 National Statistical Office of Mongolia 1999, *Yearbook 1999*, National Statistical

974 Office of Mongolia, available online at <http://www.nso.mn>

975 National Statistical Office of Mongolia, 2005. *Yearbook 2005*, National Statistical

976 Office of Mongolia, available online at <http://www.nso.mn>

977 National Statistical Office of Mongolia, 2007. *Yearbook 2007*, National Statistical

978 Office of Mongolia, available online at <http://www.nso.mn>

979 National Statistical Office of Mongolia, 2009. *Yearbook 2009*, National Statistical

980 Office of Mongolia, available online at <http://www.nso.mn>

981 Onda, Y., Kato, H., Tanaka, Y., Tujimura, M., Dvaa, G., Oyunbaatar, D., 2007.

982 Analysis of runoff generation and soil erosion processes by using environmental

983 radionuclides in semiarid areas of Mongolia, *J. Hydrol.*, 333, 124-132,

984 doi:10.1016/j.jhydrol.2006.07.030.

985 Ozyurt, N.N., Bayari, C.S., 2005. LUMPED Unsteady: a Visual Basic code of

986 unsteady-state lumped-parameter models for mean residence time analyses of

987 groundwater systems, *Computers Geosci.*, 31, 329-341.

988 Pederson, N., Jacoby, G. C., D'Arrigo, R. D., Cook, E. R., Buckley, B. M., Dugarjav, C.,

989 Mijidorj, R., 2001. Hydrometeorological reconstructions for northeastern Mongolia

990 derived from tree rings: 1651-1995, *J. Climate*, 14, 872-881.

991 Pratt M., Rasmussen, G.A., 2001. *Determining Your Stocking Rate*. Utah State

992 University Extension Electric Publishing, NR/RM/04, 7p.

993 Rathod, K. S., Rushton, K.R., 1991. Interpretation of pumping from two-zone Layered

994 aquifers using a numerical model, *Groundwater*, 29, 499-509. doi:

995 10.1111/j.1745-6584.1991.tb00541.x

996 Sasaki T., Okayasu, T. Jamsran, U., Takeuchi, K., 2008. Threshold changes in

997 vegetation along a grazing gradient in Mongolian rangelands, *J. Ecol.*, 96, 145-154,

998 doi: 10.1111/j.1365-2745.2007.01315.x.

999 Sato, T., Kimura, F., Kito, A., 2007. Projection of global warming onto regional

1000 precipitation over Mongolia using a regional climate model. *J. Hydrol.*, 333,

1001 144-154, doi: 10.1016/j.jhydrol.2006.07.023

1002 Satoh, T., Sugita, M., Yamanaka, T., Tsujimura, M., Ishii, R., 2012. Water dynamics

1003 within a soil-vegetation-atmosphere system in a steppe region covered by shrubs

1004 and herbaceous plants, in: Yamamura N, Fujita N, Maekawa A (eds), *The*

1005 *Mongolian Network: Environmental Issues under Climate and Social Changes.*

1006 *Ecological Research Monographs*, 43-63, Springer, Tokyo.

1007 Scanlon, B.R., Keese, E., Flint, L., Flint, L.E., Gaye, C.B., Edmunds, W. M., Simmers,

1008 I., 2006. Global synthesis of groundwater recharge in semiarid and arid regions.

1009 *Hydrol. Processes*, 20, 3335–3370, doi: 10.1002/hyp.6335.

- 1010 Sharkhuu, Ts., 1975. *The Situation of Land Communication Before the Revolution in*
 1011 *Mongolia*. (Хувьсгалын өмнөх Монгол дахь газрын харилцаа, Улсын
 1012 хэвлэлийн газар), State Publication House, 252p (in Mongol)
- 1013 Shiirevdamba, Ts., 1998. *Biological Diversity in Mongolia, First National Report*,
 1014 Ministry of Nature and Environment, 106p. Ulaanbaatar, Mongolia: Admon
 1015 Printing House.
- 1016 Sternberg, T., 2008. Environmental challenges in Mongolia's dryland pastoral landscape.
 1017 *J. Arid Environ.*, 72, 1294-1304. doi:10.1016/j.jaridenv.2007.12.016
- 1018 Sugita, M., Asanuma, J., Mariko, S., Tsujimura, M., Kimura, F., Lu, M., Azzaya D. and
 1019 Adyasuren Ts., 2007. An Overview of the Rangelands Atmosphere Hydrosphere
 1020 Biosphere Interaction Study Experiment in Northeastern Asia (RAISE). *J. Hydrol.*,
 1021 doi:10.1016/j.jhydrol.2006.07.032.
- 1022 Toda, M. Sugita, M., 2003. Single level turbulence measurements to determine
 1023 roughness parameters of complex terrain, *J. Geophys.Res.*, 108, D12, 4363, doi:
 1024 10.1029/2002JD002573
- 1025 Tsogtbaatar, J. Janchivdorj, L., 2009. *The Final Report of the Project on*
 1026 *"Determination of Heavy Metal in Surface Water and Groundwater of Mongolia"*,
 1027 Institute of Geoecology, Mongolian Academy of Sciences, 60p.
- 1028 Tsujimura, M., 2007. How much groundwater is available in a well, *Bull.*
 1029 *Terr. Environ. Res. Ctr., Univ. Tsukuba*, No.8 Supplement, 82-83.
- 1030 Tuinhof, A., Nemer, B., 2009, *Groundwater Assessment in the Gobi Region: Final*
 1031 *Draft Report 25/01/2009*. Acacia Water, 56p. and Annex 1-7.
- 1032 Watanabe, K. Wake, T., 2009. Measurement of unfrozen water content and relative
 1033 permittivity of frozen unsaturated soil using NMR and TDR, *Cold Regions Sci.*
 1034 *Technol.*, 59, 34-41.
- 1035 Wilson, K.B., Goldstein, A.H., Falge, E., Aubinet, M., Baldocchi, D., Berbigier, P.,
 1036 Bernhofer, Ch., Ceulemans, R., Dolman, H., Field, C., Grelle, A., Law, B., Meyers,
 1037 T., Moncrieff, J., Monson, R., Oechel, W., Tenhunen, J., Valentini, R., Verma, S.,
 1038 2002. Energy balance closure at FLUXNET sites. *Agricul. For. Meteorol.*, 113,
 1039 223–243.
- 1040 WMO (World Meteorological Organization), 2012. *Standardized Precipitation Index;*
 1041 *User Guide*, WMO-No.1090, World Meteorological Organization, Geneva.
- 1042 Yamanaka, T, Kaihotsu, I, Oyunbaatar, D., 2003. Temperature effect on soil water
 1043 content measured by time domain reflectometry and its correction using in situ
 1044 data. *Bull. Terr. Environ. Res. Ctr., Univ. Tsukuba*, 16, 246-254 (in Japanese).
- 1045 Yamanaka, T., Kaihotsu, I., Oyunbaatar, D., Ganbold, T., 2007. Summertime soil

1046 hydrological cycle and surface energy balance on the Mongolian steppe, *J. Arid*
1047 *Environ.*, 69, 65-79.

1048 Yamanaka, T., Shimada, J., Tsujimura, M., Lorphensri, O., Mikita, M., Hagihara, A,
1049 Onodera, S., 2011. Tracing a confined groundwater flow system under the pressure
1050 of excessive groundwater use in the Lower Central Plain, Thailand. *Hydrol.*
1051 *Processes*, 25, 2654-2664. doi:10.1002/hyp.8007.

1052 Yoshikawa, K., Overduin, P.P., 2005. Comparing unfrozen water content measurements
1053 of frozen soil using recently developed commercial sensors. *Cold Regions Sci.*
1054 *Technol.*, 42, 250-256.

1055

1056

1057

Table 1 A list of variables measured at the two stations.

Variable	Station	Height (m)	Sensor	Remarks
Wind speed	MG1	3.0	R.M. Young, 3101	No measurements in April-July of 2009 (see Appendix)
Temperature and relative humidity	MG1	2.65	Campbell Scientific, 41003-5 and Vaisala, HMP45D	The probe is housed in a radiation shield that has natural ventilation
Radiation	MG1	2.5	Hukseflux Thermal Sensors, NR01	Four radiation components (up and down, short and long-wave)
	MG2	2.5	Hukseflux Thermal Sensors, RA01	Two components (upward only)
Soil heat flux	MG1	-0.01	Hukseflux Thermal Sensors, HFP01	
Rainfall	MG1	0.6	Texas Electronics, TR-525M	Tipping bucket rain gauge
Soil water content (SWC)	MG1	-0.05, -0.1, -0.2, -0.3, -0.7, -1.1 (under a <i>Caragana</i> mound) and -0.05, -0.1, -0.2, -0.3, -0.5, -0.7, -1.1 (only from 2010/5, under <i>Allium</i> surface)	Campbell Scientific, CS-616	Time domain reflectometry (TDR) sensor
	MG2	-0.1, -0.2, -0.3, -0.5, -0.7		
Soil temperature	MG1	-0.1, -0.3, -0.7		Platinum resistance thermometer
	MG2	-0.1, -0.2, -0.3, -0.5, -0.7		

Table 2 Number of livestock in 2008 and assumed unit water consumption.

	W1 (heads)	W2 (heads)	Saintsagaan Soum (heads)	Unit water consumption (L head ⁻¹ day ⁻¹)
Sheep	73	200-230	94,024	4
Goats	151	200-300	107,575	4
Horses	0	14	8,732	29
Cattle	0	0	2,794	31
Camels	0	16-20	761	60

Table 3 Annual water balance for the three selected years.

Period	I		II		III		Average of periods I, II and III	
	2008/7/8-2009/7/7		2009/5/4-2010/5/3		2010/7/3-2011/7/2		W1	W2
	W1	W2	W1	W2	W1	W2	W1	W2
P	95.5		87.5		95.8		92.9	
E	65.1 (68)		83.7 (96)		80.7 (84)		76.5 (82)	
G_{out}	0	4×10^{-5} (10^{-5})						
R_{out}	0	0-0.3 (0-0.3)	0	0	0	0-0.3 (0-0.3)	0	0-0.2 (0-0.2)
U	$9.6 \cdot 10^{-2}$ (10^{-1})							
ΔS	28.8 (30)		28.0 (32)		-18.7 (-20)		12.7 (14)	
ε	1.2-1.5		-24.3		33.4-33.7		3.3 ~ 3.6	
PE	1160.0		1038.3		1029.5		1075.9	

The unit is mm a^{-1} and the percentage of each component to total P is given in parentheses. The error, ε , was determined by $\varepsilon = P - E - G_{out} - R_{out} - U - \Delta S$. The range of R_{out} for W2 is given for the assumed case of (1) with a depth, $h = 0.02$ cm, a duration, $t = 1$ h; (2) with a $h = 0.10$ cm and a $t = 3$ h; and both with a threshold rainfall intensity of $P_i = 4 \text{ mm } 10 \text{ min}^{-1}$.

Table 4 Values of $P-\Delta S$, mean storage, \bar{S} , and mean residence time, \bar{t} , estimated for the various soil layers.

MG1				MG2			
Depth (m)	$P-\Delta S$ (mm)	\bar{S} (mm)	\bar{t} (days)	depth (m)	$P-\Delta S$, (mm)	\bar{S} (mm)	\bar{t} (days)
0-0.075	56.7 (70.4)	4.7	25				
0-0.15	62.6 (77.7)	9.4	49	0-0.15	58.5 (87.6)	6.9	36
0-0.25	68.5 (85.1)	14.8	78	0-0.25	60.9 (91.3)	10	52
0-0.5	80.3 (99.8)	32	167	0-0.4	62.8 (94.5)	15.9	83
0-0.9	80.1 (99.5)	58.8	308	0-0.6	64.0 (95.8)	20.2	106
0-1.3	80.5 (100)	87.2	457	0-0.8	66.8 (100)	27.8	145

The number inside parentheses indicates the percentage of $P-\Delta S$ for each depth range to $P-\Delta S$ for the largest depth range for each station. $P-\Delta S$ was determined for 2009/5/4-2010/3/8 for the MG1 station, and for 2009/5/4-2010/3/31 for the MG2 station in order to avoid periods with possibly large errors for $P-\Delta S$. The mean residence time was estimated by $\bar{t} = \bar{S} / \bar{P}$ where \bar{P} is mean daily precipitation.

Table 5 Results based on the tritium analysis of well water.

	C (TU)	C_0 (TU)	\bar{t} (years)	\bar{q}_z (mm a ⁻¹)
GW1	17.19±2.32	80-200	28-44	9.5-15
GW2	3.70±1.50	50-100	47-59	7.1-8.9
GW4	7.76±1.34	50-100	34-46	9.1-12

C is the tritium concentration of sampled well water, C_0 is the estimated tritium concentration of groundwater at the time of recharge, \bar{t} is the mean residence time of shallow groundwater derived from (A.5), and \bar{q}_z is the mean recharge rate to shallow groundwater estimated by

$$\bar{q}_z = \bar{S} / \bar{t}.$$

1058 Figure caption

1059 Figure 1 The topography of the study area. Closed circles indicate the locations of
1060 automatic weather stations (AWS) MG1 and MG2 and wells GW1-GW4. Watersheds
1061 boundaries are shown with dotted lines, while contours are given by continuous lines at
1062 10 m intervals. The smaller watershed located to the east is W1 and the larger
1063 watershed to the west is W2. Also shown as an inset is a map of Mongolia with aimag
1064 (prefecture) boundaries and capital cities, and those of the surrounding area of the two
1065 watersheds. The study area is located near Mandalgobi in Dundgobi Aimag (shown in
1066 the map as a red circle with a center dot and as the shaded area).

1067

1068 Figure 2 The time change for groundwater level (GWL, m asl), soil temperature (T_{soil})
1069 at a depth of 10 cm, soil water content (SWC), and the accumulated values of E , P , and
1070 $P-\Delta S$ in which ΔS in this case was determined from SWC data obtained from the
1071 surface down to -1.3 m. All values were obtained from the MG1 AWS station, with
1072 the exception of GWL. Some of the MG1 AWS station data were not available for the
1073 period of 2010/5/12-7/2, due to a technical problem, and, thus, the accumulated lines of

1074 E , P , and $\sum P-\Delta S$ were reset to zero. The dotted line for SWC data is for
1075 measurements under an *Allium* surface. The depth of the sensor is indicated by the color
1076 of each line.

1077

1078 Figure 3 Changes in livestock number in Saintsagaan soum and the number of wells
1079 within Mongolian pastureland based on the National Statistical Office of Mongolia
1080 (1999, 2005, 2007, and 2009).

1081

1082 Figure A1 The time variation for the precipitation tritium concentration (open circles)
1083 and groundwater (closed triangles). Dotted lines represent the decay function
1084 $N = N_0 \exp(-\lambda t)$ through the tritium concentration for water samples from GW1,
1085 GW2, and GW4 during 2011. t is the elapsed time and N is the number of nuclides in
1086 T.U., λ is the decay constant, and N_0 is N at an initial time of $t = 0$.

1087

Fig. 1

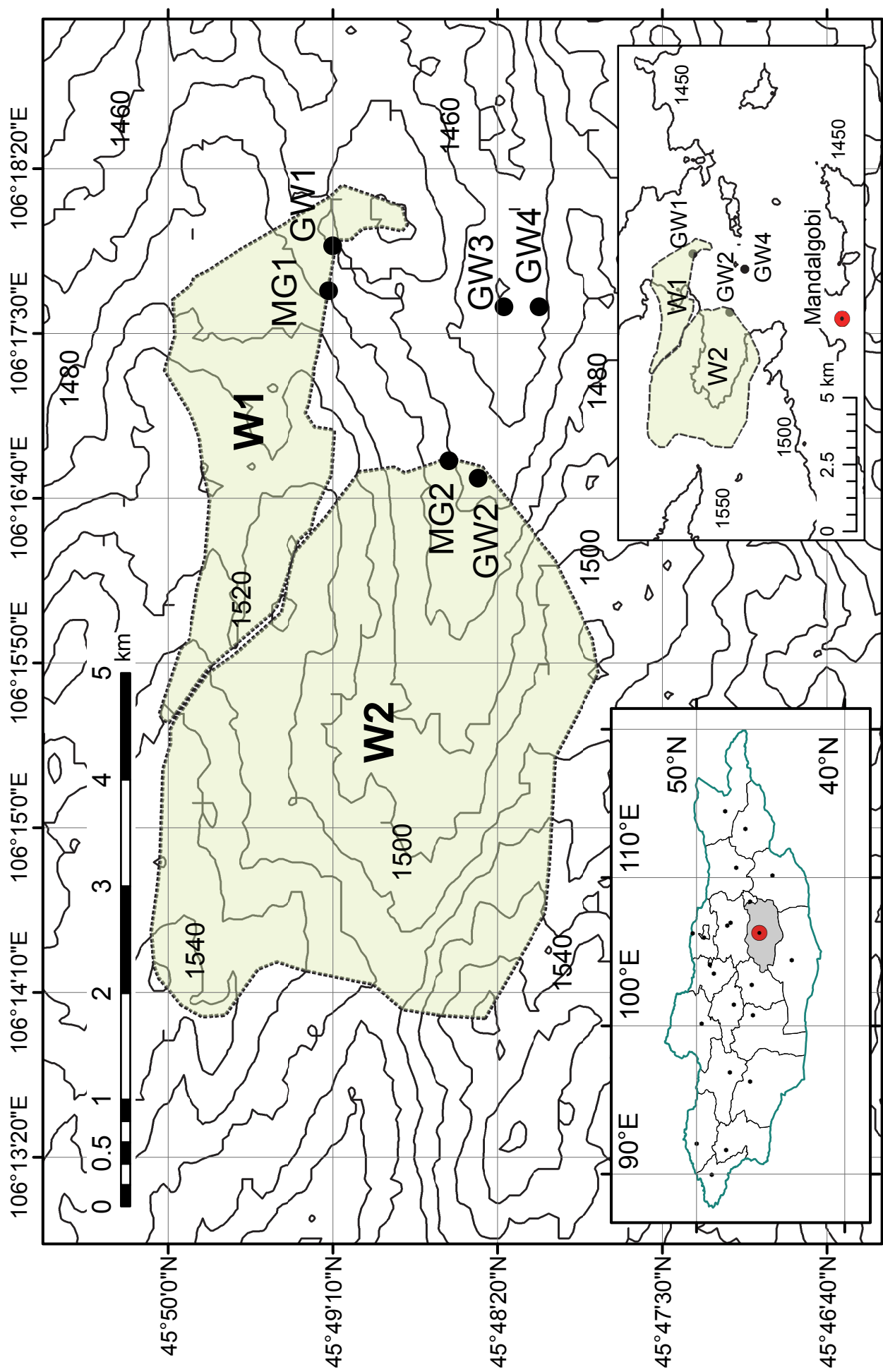


Fig. 2

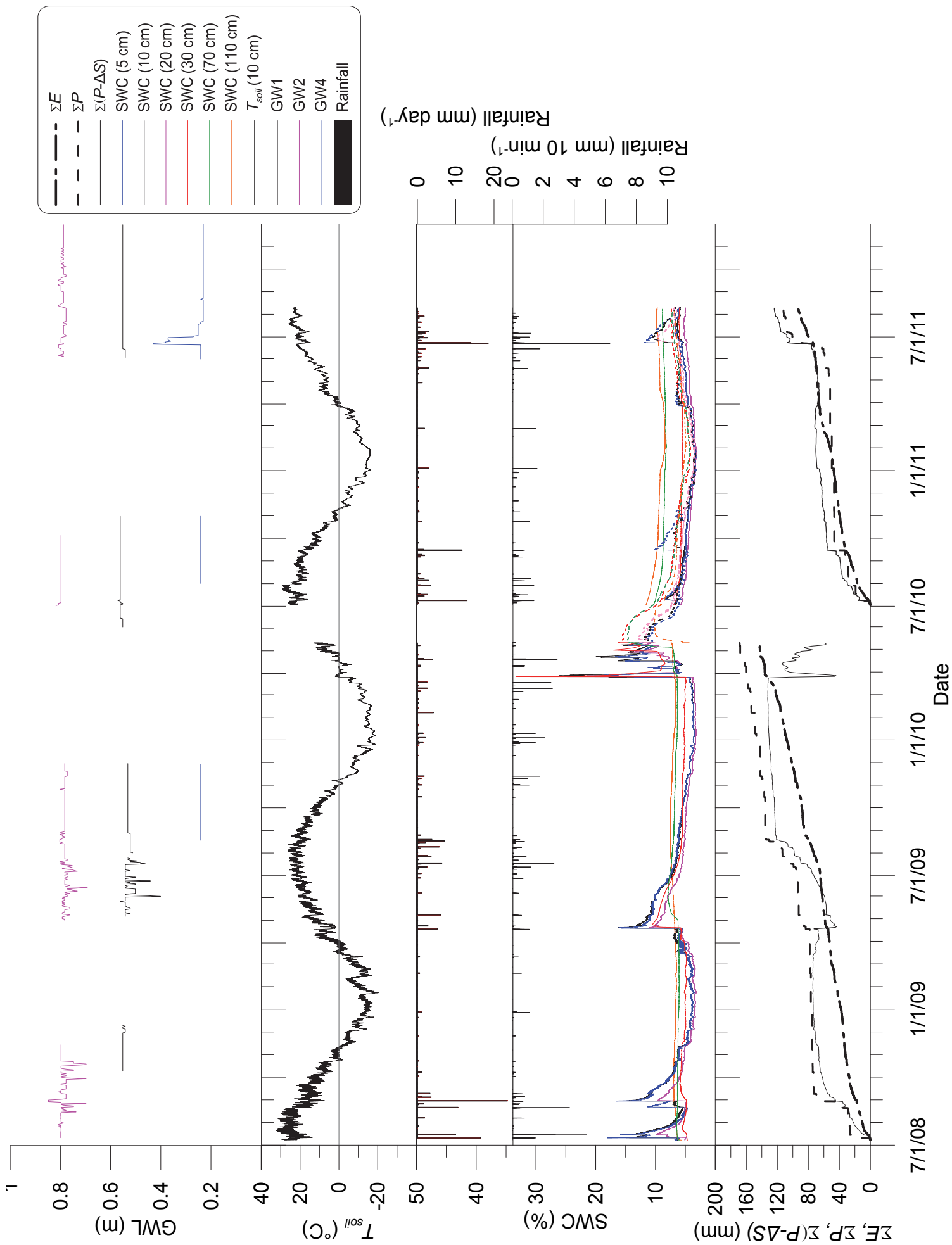


Fig. 3

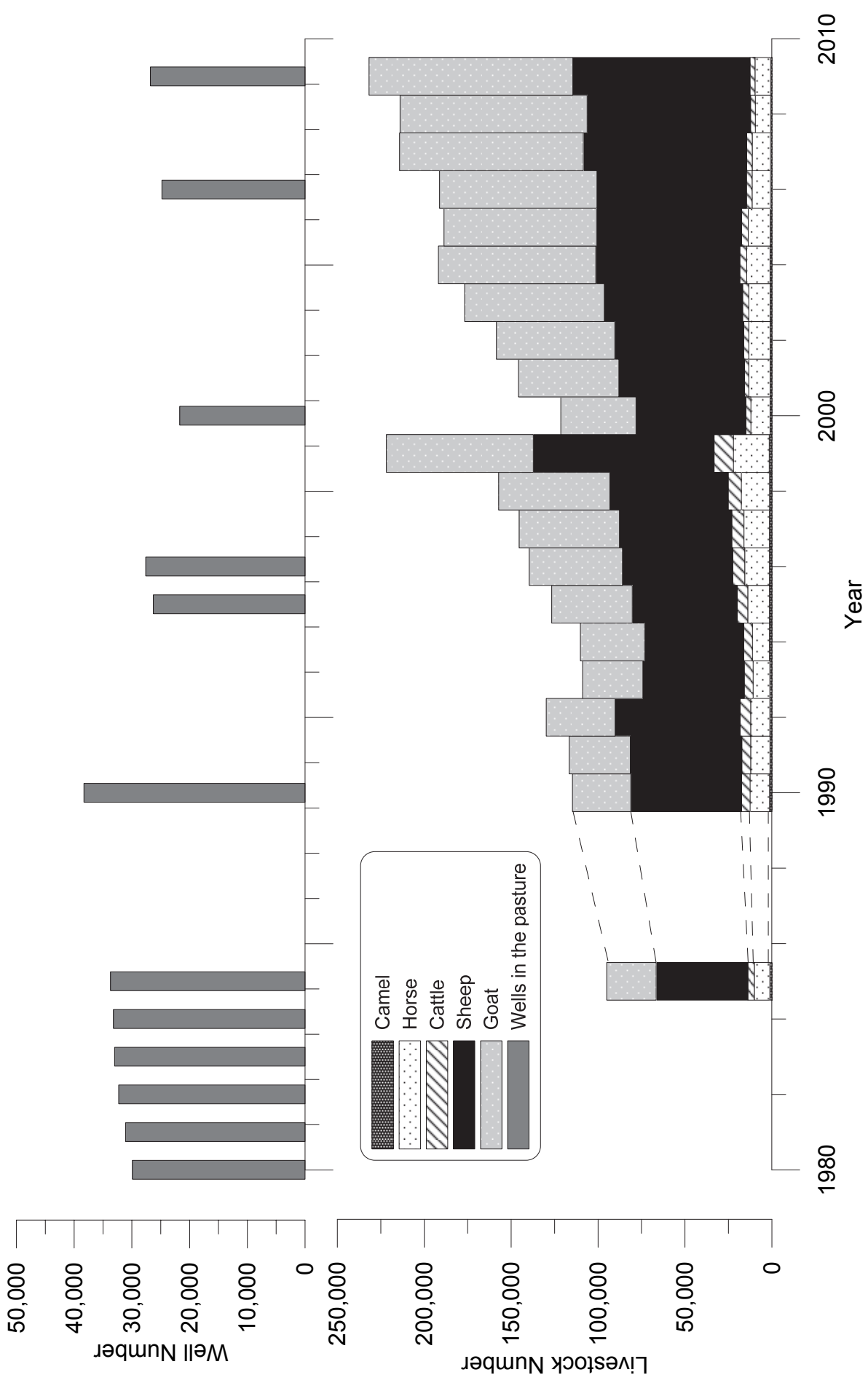


Fig. 4

